Nuclear Inst. and Methods in Physics Research, A 964 (2020) 163788

Contents lists available at ScienceDirect

Nuclear Inst. and Methods in Physics Research, A

journal homepage: www.elsevier.com/locate/nima

Technical Notes

Reduction of waveguide vacuum trips in CEBAF accelerating cavities with a combination ion pump and non-evaporable getter pump

G. Ciovati *, M. Drury, J. Fischer, M. Stutzman, S. Suhring

Thomas Jefferson National Accelerator Facility, Newport News, VA 23606, USA

ARTICLE INFO

Keywords:
Vacuum
Waveguide
NEG pump

ABSTRACT

Pressure spikes in the fundamental power coupler waveguide are a significant source of trips during the operation of both original and refurbished superconducting radio-frequency cavities installed in the CEBAF accelerator. In its original configuration, two waveguides from a cavity-pair are connected to a single 32 l/s ion pump. In 2017 a new cavity-pair was installed in a refurbished cryomodule in which a NEXTorr® D200-5 combination ion pump and non-evaporable getter pump was installed for each waveguide. It is shown that hydrogen is the dominant residual gas in the waveguide and simulations with Molflow+ indicated that the new pumping scheme allows reducing the pressure at the end of the waveguide by a factor of ∼ 5, compared to the original configuration. The new cavity-pair has been operating in CEBAF for a total of 431 days and it only had a total of 3 trips due to vacuum spikes in the waveguide.

1. Introduction

The Continuous Electron Beam Accelerator Facility (CEBAF) is a continuous-wave electron accelerator which has been operating at Jefferson Lab since 1994 [1]. Acceleration of the electron beam is provided by four hundred and eighteen 1497 MHz superconducting radio-frequency (SRF) cavities cooled to a temperature of 2.07 K. Eighty cavities, named "C100" are 7-cells cavities installed since 2010 and designed to operate at an accelerating gradient of 19.7 MV/m [2]. One hundred and four cavities, named "C50", are 5-cell cavities from the original installation, but they have been refurbished between 2007 and 2017 with up-to-date surface processing methods and are designed to operate at an accelerating gradient of 12.5 MV/m [3]. The remaining cavities, labeled "C20", are 5-cell cavities from the original installation and they were designed to operate at an accelerating gradient of 5 MV/m. RF power from klystrons is provided to each cavity through a rectangular fundamental power coupler (FPC) waveguide. The maximum available klystron power is 13 kW for a C100 cavity and 4 kW for the other cavities, except a few C50 cavities which are powered by 8 kW klystrons.

In C20 and C50 cryomodules, eight cavities are divided into four pairs, with each pair installed in a common liquid helium vessel. A schematic of a C20 cavity pair cryounit is shown in Fig. 1 [4]. For each cavity, a ceramic RF window brazed to a stainless steel flange of the fundamental power coupler (FPC) cavity waveguide is sealed to the helium vessel and it isolates the ultra-high vacuum inside the cavity pair from the atmospheric pressure outside of the helium vessel during the assembly of the cryomodule or the high-vacuum inside the vacuum vessel, after completion of the cryomodule assembly. Since the inside of the helium vessel is filled with liquid helium at 2.07 K, this ceramic window is referred to as the "cold window".

A copper-plated stainless steel rectangular waveguide with 2.54 cm × 13.3 cm cross section is mounted between the cold window and the vacuum vessel. A copper block is brazed approximately mid-way along the waveguide and thermal straps are used to connect it to the cryomodule's heat shield. A copper-plated waveguide extension with the same cross section as the waveguide itself is attached to the vacuum vessel and it ends with a ceramic RF window brazed into a stainless steel flange to isolate the high-vacuum inside the waveguide from the atmospheric pressure outside the cryomodule. This ceramic window is at room temperature and is referred to as the "warm window". The approximate length of the rectangular waveguide between the two RF windows is 48 cm. Two ports in the narrow side of the waveguide extensions are used for an arc detector and for an infrared sensor to monitor the temperature of the cold window. A side port with a 70 mm diameter ConFlat® flange is used for the connection to the vacuum pump. A picture of the 48 cm long waveguide section is shown in Fig. 2

Two stainless steel vacuum tubes with 3.5 cm inner diameter connect the two waveguide ports through a tee to a Perkin-Elmer noble diode ion pump with a nominal pumping speed for hydrogen of 32 l/s, as shown in the picture in Fig. 3. Unlike for C20/C50 cryomodules, the vacuum in the FPC waveguide of each C100 cavity is maintained by a 35 l/s ion pump mounted close to the waveguide. As it will be

* Corresponding author.
E-mail address: gciovati@jlab.org (G. Ciovati).

https://doi.org/10.1016/j.nima.2020.163788
Received 17 February 2020; Received in revised form 10 March 2020; Accepted 10 March 2020
Available online 16 March 2020
0168-9002/

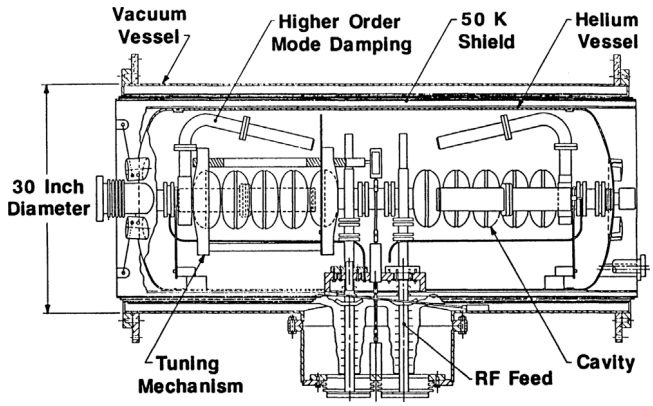

Fig. 1. Schematic of the cryounit of an original C20 CEBAF cryomodule [4].

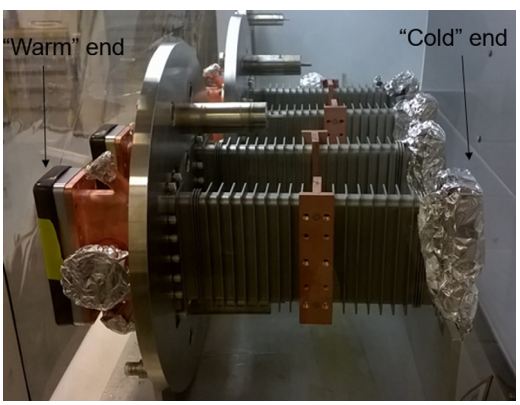

Fig. 2. Picture showing an FPC waveguide section between the warm and the cold RF windows.

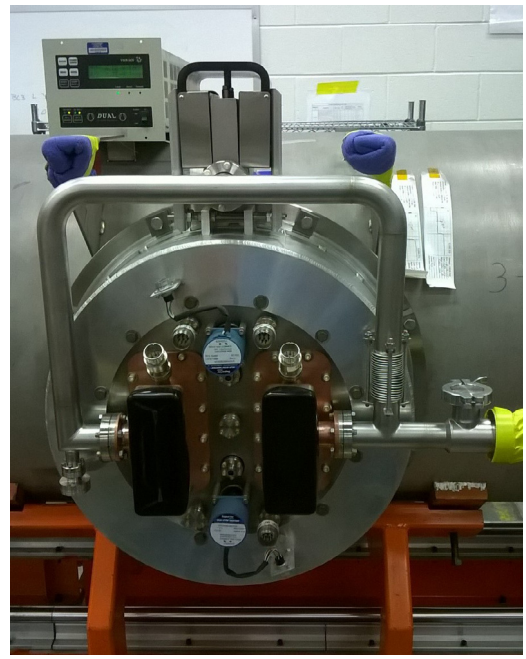

Fig. 3. Picture showing the ion pump and the vacuum manifold connected to two FPC waveguides of a cavity pair in C20/C50 cryomodules.

Table 1
Number of faults for different categories during the operation of C20, C50 and C100 cavities in CEBAF from January 2nd, 2015 to March 3rd, 2017.

C20	
Fault type	Count (%)
TRUEARC	41991 (53%)
ARC	7844 (10%)
CWV	8595 (11%)
QUENCH	14348 (18%)
CWWT	5949 (8%)
C50	
Fault type	Count (%)
TRUEARC	843 (5%)
ARC	1161 (6%)
CWV	3299 (19%)
QUENCH	11778 (67%)
CWWT	586 (3%)
C100	
Fault type	Count (%)
CWAD	257 (2.7%)
CWV	34 (0.4%)
QUENCH	8938 (93.7%)
CWWT	310 (3.2%)

shown in Section 2, pressure spikes in the FPC waveguide are a significant cause for trips in C20/C50 cryomodules. Since 2017, the plan for the refurbishment of original CEBAF cryomodules was updated to produce "C75" cryomodules, in which the cavities would be operating at an accelerating gradient of 19.1 MV/m by manufacturing new 5-cell structures with large-grain Nb [5]. New 8 kW klystrons will be used for C75 cryomodules. In order to minimize the potential for vacuum spikes during the operation of the future C75 cryomodules, a solution was studied in which the common ion pump is replaced by a compact non-evaporable getter (NEG) and ion combination pump for each FPC waveguide. A study of the residual gases in the FPC waveguide during operation of a C50 cavity is shown in Section 3 and the results from simulations using Molflow+ are described in Section 4. The results from the operational experience of a cavity pair with the new FPC waveguide pumping configuration are reported in Section 5.

2. Operational limitations of CEBAF cavities

Table 1 lists the number of faults by category during the operation of C20, C50 and C100 cavities from January 2nd, 2015 to March 3rd, 2017, corresponding to 328 days of operations of CEBAF. The fault categories are: temperature of the cold window in the FPC waveguide (CWWT), arcing at the cold window (CWAD), pressure in FPC waveguide (CWV) and quench. For C20 and C50 cryomodules a fault from the arc detector (ARC) is distinguished from a simultaneous fault from both the arc detector and the pressure in the FPC waveguide, which is referred to a "true arc" (TRUEARC). The average trip rate during the timeframe considered is ~0.4 faults/cavity/day for C100 cavities, ~1.0 faults/cavity/day for C20 cavities and ~0.6 faults/cavity/day for C50 cavities. It should be noted that a fault due to high FPC waveguide pressure is assigned to two cavities of a pair in C20/C50 cryomodules, since they share the same vacuum space, even if the fault occurs in one cavity only. Such duplicates have been removed in the count shown in Table 1. The FPC waveguide interlock is set to 5×10^{-7} Torr for C20 and C50 cavities and 1×10^{-7} Torr for C100 cavities.

The major limit of the operation of C20 cavities is the occurrence of arcs at the cold window and it was found that this was due to charging of the window by field emitted electrons from the cavity [6]. In C50 cryomodules, a curved waveguide section was installed inside the helium vessel, between the cavity and the cold rf window, to avoid line-of-sight between the window the cavity. As a result the trip rate due to arcing was reduced substantially in C50 cryomodules, which are dominated by quenching of the cavities. Quenching of the cavities results from operating them close their maximum limit, typically given

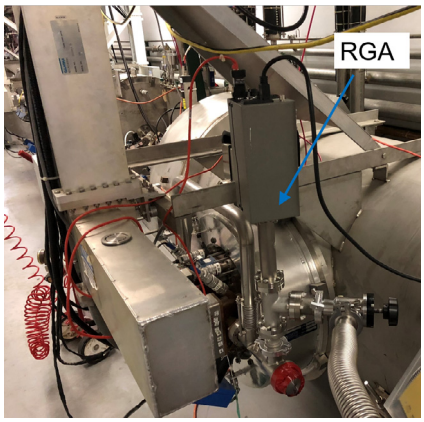

Fig. 4. Picture showing the RGA installed on the vacuum manifold connected to two FPC waveguides of a cavity pair in the C50 cryomodule in zone 1L04 in CEBAF.

by a thermal breakdown induced by rf heating of a defect inside the cavity surface of by heating due to field emitted electrons impinging on the cavity surface. A significant fraction of faults in C50 cryomodules is due to pressure spikes in the FPC waveguide, although the fault distribution is not uniform among such cryomodules.

Unlike for C20/C50 cryomodules, faults due to pressure spikes in the FPC waveguide of C100 cavities is negligible, even though they handle a higher RF power than those of C20/C50 cryomodules.

3. Analysis of residual gases in the FPC waveguide during operation

In order to investigate the evolution of residual gases in the FPC waveguide during the operation of a C50 cavity, a residual gas analyzer (RGA) was installed on the vacuum manifold connected to the FPC waveguides of the cavity pair 1L04-1/2 of the C50 cryomodule installed in zone 1L04 in CEBAF (Fig. 4). The temperature profile along the FPC waveguide measured in one of the C50 cryomodules during operations showed that the cold end of the waveguide is at ~ 4 K and the section between the heat station and the cold end is at ~ 50 K. The cavity 1L04-1 was operated at a gradient of ~ 14 MV/m between November 10th, 2017 and November 13th, 2017. During this time it had a total of six CWV faults associated with spikes in the hydrogen pressure, as shown for example in Fig. 5. The cavity recovered from each trip within few seconds.

The cavity 1L04-2 was operated at a gradient of 12–14 MV/m between November 13th, 2017 and November 15th, 2017 and a total of 66 faults, CWV and TRUEARC, occurred during this time period. The cavity recovered from each trip within few seconds. Fig. 6 shows the partial pressure of the residual gases in the FPC waveguides vacuum manifold measured on Nov. 14th, 2017 in a time period when several faults occurred: a spike in all residual gases occurred during arcing events whereas hydrogen spikes corresponded to CWV faults. In some cases spikes in He pressure occurred as well.

4. New pumping configuration and Molflow+ simulations

The data shown in Section 3 show that hydrogen is the main residual gas in the FPC waveguide and the one causing pressure spikes, resulting in trips of the accelerating cavity. This finding perhaps is not surprising since a large section of the waveguide is at cryogenic temperature and all other residual gases would be adsorbed on the cold surfaces. A possible solution to reduce the partial pressure of hydrogen is to utilize NEG pumps which are compact and allow large pumping speeds. A small ion pump would still be beneficial to have in order to pump noble gases, such as helium, which might result from a leak at

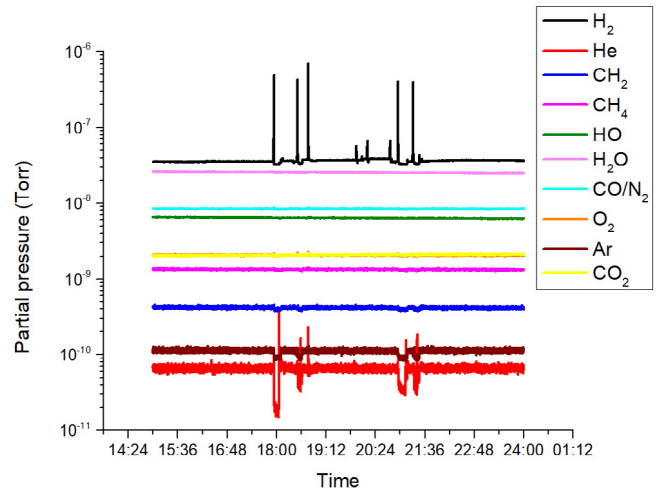

Fig. 5. Partial pressures during the operation of cavity 1L04-1 at ~ 14 MV/m on Nov. 12th, 2017. The spikes in the hydrogen pressures correspond to spikes in the pressure in the cavity pair FPC waveguide and caused CWV trips of the cavity.

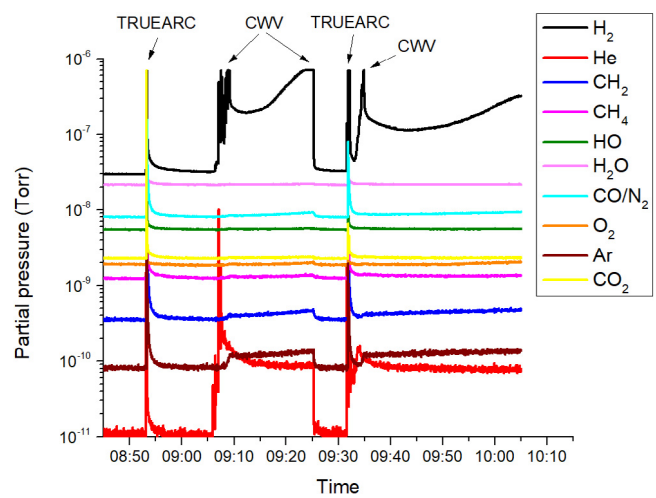

Fig. 6. Partial pressures during the operation of cavity 1L04-2 at ~ 14 MV/m on Nov. 14th, 2017.

the joint of the cold RF window to the He vessel. The pump selected for the new pumping configuration is the NEXTorr® D200-5 from SAES Getters S.p.A, Italy, which has a NEG cartridge with a nominal pumping speed of 200 l/s for H_2 and a 6 l/s (Ar) ion pump. The pump is inserted in a 35 mm diameter tee with a ConFlat flanges at the ends. In order to maximize the effective pumping speed, a separate pump is installed for each FPC waveguide. An inline valve is used to isolate the NEXTorr pump from the FPC waveguide during activation and a right-angle valve is used to connect the pump to a turbo-pump cart during activation. A picture of the proposed new pumping configuration is shown in Fig. 7.

3D models of the old and new vacuum volumes for the FPC waveguide of C20/C50 cryomodules were imported in the test-particle Monte Carlo simulator Molflow+ [7] to calculate the hydrogen pressure distribution and effective pumping speed. For the old configuration a half-model was considered due to symmetry. Fig. 8 shows the pressure distribution for the old and new configurations, respectively, when the FPC waveguide is pumped at room temperature, prior to the cryomodule cool-down. In both cases, an outgassing coefficient of 5×10^{-11} mbar l/s/cm^2 was set for all surfaces [8]. The effective pumping speed of the NEXTorr® D200-5 inside a 35 mm nipple is set to 68 l/s [9]. The

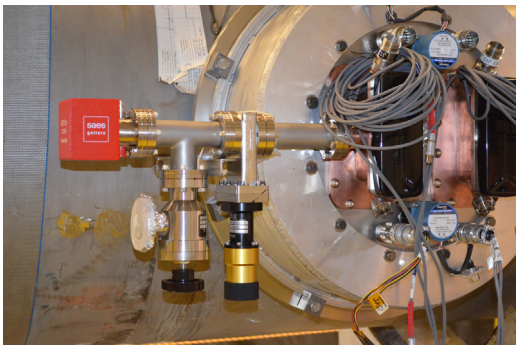

Fig. 7. Picture of the NEXTorr® D200-5 pump installed on the FPC waveguide of cryomodule C50-13.

pressure at the far end of the rectangular waveguide is $\sim 1\times10^{-9}$ mbar, about a factor of five lower than in the old configuration.

Fig. 9 shows the pressure distribution for the old and new configurations, respectively, simulating the case when the cavities are at the operating temperature of 2.07 K with ~3 kW of forward RF power into the FPC waveguide. The temperature along the FPC waveguide was measured in several locations in a C50 cavity and the data was used to assign different temperatures along the waveguide, as shown in Fig. 9(b) for both old and new pumping configurations. A sticking coefficient $\sigma = 0.1$ was assigned to the cold surface at 4 K at the far end of the rectangular waveguide [10]. Surfaces with temperature between 50 – 230 K were assigned both zero outgassing and zero sticking. The same outgassing coefficient as for the room temperature case of Fig. 8 was assigned to all other surfaces at 293 K. The pressure along the waveguide is lower in the new configuration by about 50%, compared to the old configuration.

5. Outcome from operation with the new pumping configuration

The new pumping configuration (Fig. 7) using the NEXTorr® D200-5 pump was installed on the FPC waveguides of a C75 prototype cavity pair, installed in the cryomodule C50-13 which has been operating in CEBAF in zone 1L13 since November 2017. The remaining three cavity pairs in 1L13 are standard C50 cavities with the old pumping configuration. The pressure measured in the FPC waveguides at 295 K, prior to cooldown, was 6×10^{-10} mbar for the new pumping configuration, compared to an average of $\sim 1.7\times10^{-8}$ mbar for the old pumping configuration. After cooldown to 2.07 K, the pressure in the FPC waveguides decreased to 3×10^{-10} mbar and 1×10^{-9} mbar for the new and old pumping configurations, respectively. Fig. 10(a) shows a hystogram of the waveguide vacuum faults that occurred in cryomodule 1L13 between November 26th, 2017 and September 8th, 2019, corresponding to 431 days of operation. Fig. 10(b) shows the average accelerating gradient that each cavity was operated at during the same period of time. Cavities 1 and 2 were the ones which had the new pumping configuration installed on the FPC waveguides. The data show that cavity 1 only had two trips due to CWV and cavity 2 only one such trip, significantly smaller than an average of 42 trips/cavity in the remaining six cavities, whereas all of the cavities had been operating at a comparable accelerating gradient.

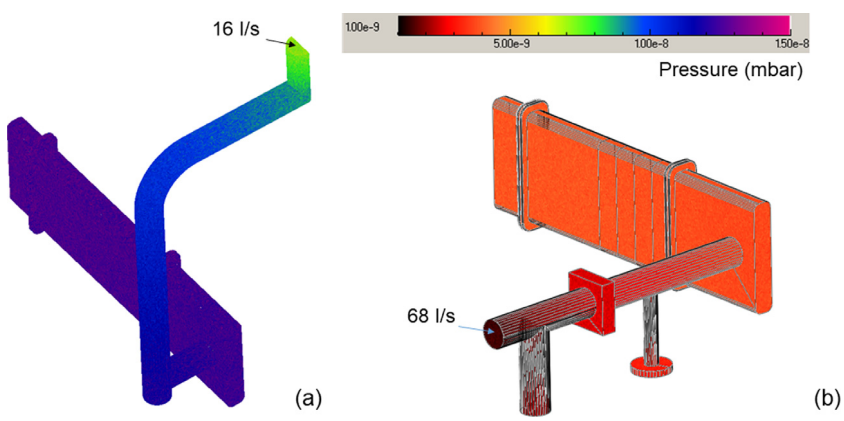

Fig. 8. Results of Molflow+ simulations showing the pressure distribution in the FPC waveguide and pumping manifolds at 293 K for the old (a) and new (b) pumping configurations. The images in (a) and (b) are not to scale.

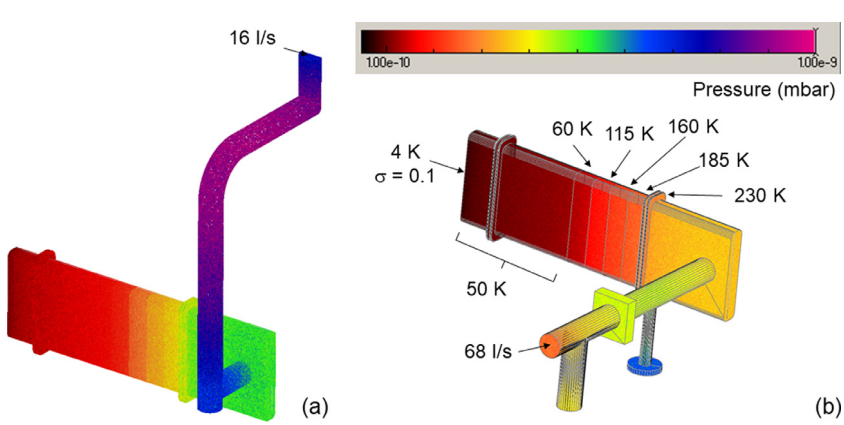

Fig. 9. Results of Molflow+ simulations showing the pressure distribution in the FPC waveguide and pumping manifolds with the cold end at 4 K for the old (a) and new (b) pumping configurations. The images in (a) and (b) are not to scale.

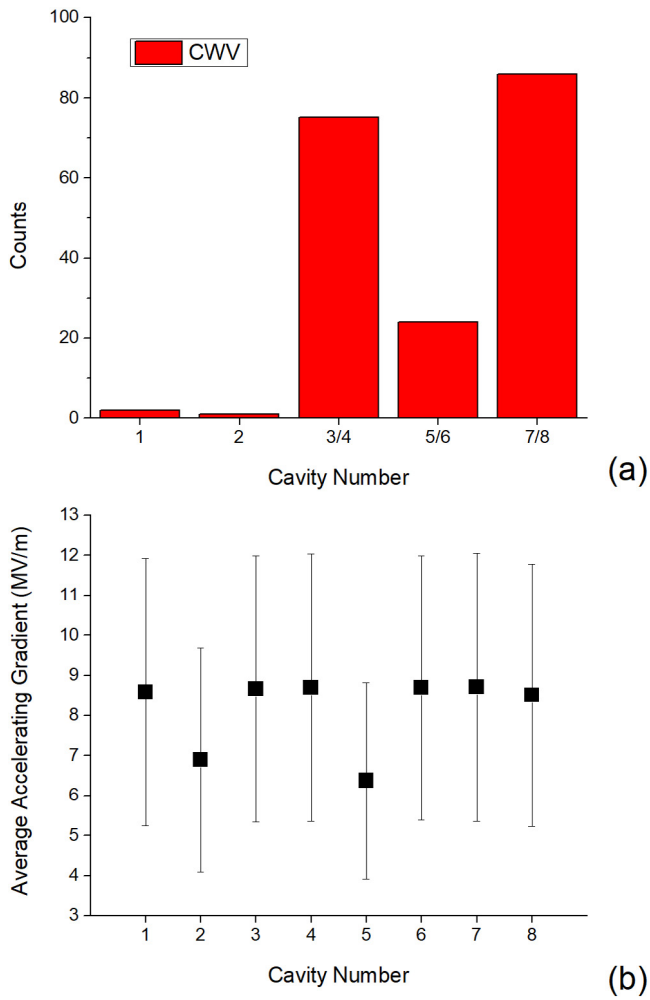

Fig. 10. Number of faults due to waveguide vacuum spikes (a) and average accelerating gradient(b) for the cavities operating in zone 1L13 for over 431 days. Cavities 1 and 2 had the new pumping configuration installed.

A possible question regarding the operation of the NEXTorr® D200-5 pump is whether the pressure measured through the ion pump section is reduced by the reduced conductance to the pump being inserted in a 35 mm diameter tee, however this effect was measured to be small, definitely not enough to mask a pressure spike of several orders of magnitude [11].

An additional test was proposed in which the pumping configuration would be updated for a cavity-pair which had significant CWV trips in a cryomodule already installed in CEBAF to check whether the performance could be improved. However such effort would require warming up of the whole cryomodule in order to bring the pressure of the FPC waveguides back to 1 atm for the required modifications to be done and such opportunity is yet to occur.

6. Conclusion

The updated plan for the refurbishment of old cryomodules in the CEBAF accelerator requires the installation of cavities operating at higher accelerating gradient and RF power than those originally installed. The previous cryomodule refurbishment program showed that pressure spikes in the FPC waveguide during operation are a significant contributor to the cavity trip rate. It has been shown that hydrogen is the gas being desorbed during the pressure spikes. A new pumping configuration utilizing an ion-NEG combination pump has been proposed and simulations indicated the ability to significantly reduce the hydrogen pressure in the FPC waveguide with such configuration. The long-term operation of two cavities in which this solution was implemented validated the design which is going to be adopted for the future refurbishment of CEBAF cryomodules.

Declaration of competing interest

The authors declare that they have no known competing financial interests or personal relationships that could have appeared to influence the work reported in this paper.

CRediT authorship contribution statement

G. Ciovati: Conceptualization, Methodology, Data curation, Formal analysis, Writing - original draft, Writing - review & editing. **M. Drury:** Formal analysis, Funding acquisition. **J. Fischer:** Supervision, Investigation. **M. Stutzman:** Conceptualization. **S. Suhring:** Supervision, Investigation.

Acknowledgments

The authors would like to thank our colleagues from Jefferson Lab, F. Humphrey and L. King for helping with the installation and data acquisition of the RGA on the FPC waveguide of 1L04 and K. Macha for providing the 3D models of the old and new pumping configurations. We would also like to thank Y. Lushtak and E. Maccallini from SAES Getters for helpful discussions. This manuscript has been authored by Jefferson Science Associates, LLC under U.S. DOE Contract No. DE-AC05-06OR23177. The U.S. Government retains a non-exclusive, paid-up, irrevocable, world-wide license to publish or reproduce this manuscript for U.S. Government purposes.

References

[1] C.W. Leemann, D.R. Douglas, G.A. Krafft, The continuous electron beam accelerator facility: CEBAF at the Jefferson Laboratory, Annu. Rev. Nucl. Part. Sci. 51 (1) (2001) 413–450, http://dx.doi.org/10.1146/annurev.nucl.51.101701.132327.

[2] A. Reilly, T. Bass, A. Burrill, G. Davis, F. Marhauser, C. Reece, M. Stirbet, Preparation and testing of the SRF cavities for the CEBAF 12 GeV upgrade, in: Proc. 15th Int. Conf. RF Superconductivity (SRF'11), JACoW, Chicago, IL, USA, 2011, pp. 542–548.

[3] M. Drury, G. Davis, J. Fischer, C. Grenoble, J. Hogan, L. King, K. Macha, J. Mammosser, C. Reece, A. Reilly, J. Saunders, H. Wang, E. Daly, J. Preble, Summary report for the C50 cryomodule project, in: Proc. 24th Particle Accelerator Conf. (PAC'11), JACoW, New York, NY, USA, 2011, pp. 1044–1046.

[4] C. Leeman, CEBAF Design overview and project status, in: Proc. 3rd Int. Conf. RF Superconductivity (SRF'87), Lemont, IL, USA, JACoW, 1987, p. SRF87A09.

[5] R. Rimmer, et al., Upgraded cavities for the CEBAF cryomodule rework program, in: Proceedings, 18th International Conference on RF Superconductivity (SRF2017), Lanzhou, China, July 17–21, 2017, JACoW, 2018, p. MOPB049, http://dx.doi.org/10.18429/JACoW-SRF2017-MOPB049.

[6] T. Powers, P. Kneisel, R. Allen, Arcing phenomena on CEBAF RF-windows at cryogenic temperatures, in: Proc. 16th Particle Accelerator Conf. (PAC'95), Dallas, TX, USA, May 1995, vol. 3, JACoW, 1995, pp. 1645–1647, http://dx.doi.org/10.1109/PAC.1995.505314.

[7] R. Kersevan, M. Ady, J.L. Pons, Molflow+ (version 2.7.7), 2019, cern.ch/molflow.

[8] K.C. Ratnakala, S.K. Tiwari, S.K. Shukla, S. Kotaiah, Outgassing rate measurement of copper plated stainless steel, J. Phys. Conf. Ser. 114 (2008) 012056, http://dx.doi.org/10.1088/1742-6596/114/1/012056.

[9] S. Wulfsberg, personal communication.

[10] Molecular desorption by synchrotron radiation and sticking coefficient at cryogenic temperatures for H2, CH4, CO and CO2, in: 7th European Vacuum Meeting/3rd European Topical Conference on Ha rd Coatings, Vacuum 67 (3) (2002) 421–428, http://dx.doi.org/10.1016/S0042-207X(02)00226-9, http://www.sciencedirect.com/science/article/pii/S0042207X02002269.

[11] Y. Lushtak, personal communication.